19th Brazilian Congress of Thermal Sciences and Engineering
November 06th-10th, 2022, Bento Gonçalves - RS - Brazil

ENC-2022-0222
MATHEMATICAL MODELLING FOR SOLAR-POWERED SEAWATER DESALINATION PROCESS ON THE SOLID OPEN-CELL FOAM BED BASED ON DIRECT CONTACT MEMBRANE (DCM): A SIMULATION STUDY

Renato da Silva Pereira
Daniel Ribeiro Dessaune
Jornandes Dias da Silva
Polytechnic School - UPE, Laboratory of Environmental and Energetic Technology; Rua Benfica - 455, Madalena, Recife – PE, Brazil, Cep: 50750-470
rsp1@poli.br
drd1@poli.br
jornandesdias@poli.br

Abstract. *Fresh water scarcity is expected to be one of the major risks for society in the future, since the global water demand is constantly increasing at around 1% pace per year achieving a nearly 30% increase by 2050 due to population growth and industrial development. Seawater desalination is a sensible choice because seawater represents more than 96 % of the total global water. The world sustainability will be severely ensured by production of clean water and new energy sources that are intimately connected in the next decades. The membrane technology has become increasingly important in separation processes and its fields of applications have been amplified in engineering processes. The solar-driven evaporation process in medium porous can be promising choice to make salt-water into freshwater from the use of Direct Contact Membrane (DCM). This work has as main aim the mathematical modelling to describe solar-driven seawater desalination process on the solid open-cell foams (β-SiC) using the DCM technology. The desalination system's variables describe the specific aims from each equation of the physical-mathematical model for characterizing the performance of the heat and mass transfer from seawater evaporation process. This study investigates the evaporation characteristics of seawater when placed on the heated DCM system to check the efficiency of solar energy utilization in solar driven fresh water generation.*

Keywords: *Modelling, Thermal polarization, Seawater, Desalination, Solar*

1. INTRODUCTION

The world's sustainability capacity will be severely stressed by clean water and energy resources that are intimately linked in the next decades. Currently, scarcity of fresh water has become one of the most serious challenges for the global development. The industrialization's advance, the rapid increase of urbanization and the improvement in life standards have raised the fresh water demand. The solar-driven desalination technology is an efficiency way of producing freshwater from seawater using the Direct Contact Membrane (DCM) for producing high quality distilled water (Ali et al., 2018). DCM distillation is a hybrid thermal-membrane system that uses a steam pressure difference created by a temperature gradient across a hydrophobic membrane (Golubev et al., 2021). Different types of renewable energy can be used to the DCM distillation, such as solar thermal energy, solar photovoltaics, wind power, and geothermal energy as discussed in the comprehensive review paper (Kalogirou, 2005). For this work, the solar thermal energy will be used to heat the thermal-membrane desalination system.

Solar-driven evaporation technology in porous medium can be emerged as a promising and sustainable approach to convert seawater into freshwater using photothermal materials with high salt adsorption on porous solids (Ying et al., 2021). Solar-driven seawater evaporation assisted by photothermal packed beds is a novel strategy to improve solar distillation. Packed beds with high porosity are effective systems for heat and mass adsorption due of their simple structure, low cost, and good heat and mass transfer performance. Due to high porosity of solid open-cell foams (for example, β-SiC), packed beds built with β-SiC are excellent thermal energy adsorbers and can be used to improve the solar light-driven evaporation process (Voltolina et al., 2017). Mass, energy and momentum balance's equations for the

fluid phase as well as mass, energy and momentum balance's equations to the solid phase are described through mathematical models (Rafiei et al., 2020). Here, the application of a heterogeneous mathematical model will be used to model the heat and mass transfer phenomena in DCM distillation system.

The present study shows a detailed mathematical model of the heat and mass transfer for solar-driven DCM distillation module. The main objective of this work is to corroborate the comparison of temperature profiles between the conventional DCM distillation module (without particles) and DCM distillation module (with particles). In addition, the permeation flux as a function of the steam temperature is also investigated.

2. PROBLEM DESCRIPTION

The schematic setup from Figure 1 shows a solar-driven DCM distillation module. In this setup, a solar collector and feed tank are coupled to the DCM distillation module through of a feed pump. In this figure, the first loop in the system is a closed loop of fluid that is heated by the solar collector and it transports the thermal energy to the hot water tank. The hot water is circled from the hot water tank into the DCM distillation module and back to the hot water tank. The permeated amount from the fresh water tank is pumped into the DCM distillation module where it collects the distilled water and flows back into the fresh water tank. The inclusion of the solar collector and hot tank allows for dynamic energy storage that can be used to improve the DCM distillation module efficiency under real operating conditions. This work focuses only on the DCM distillation module's modelling due to paper length.

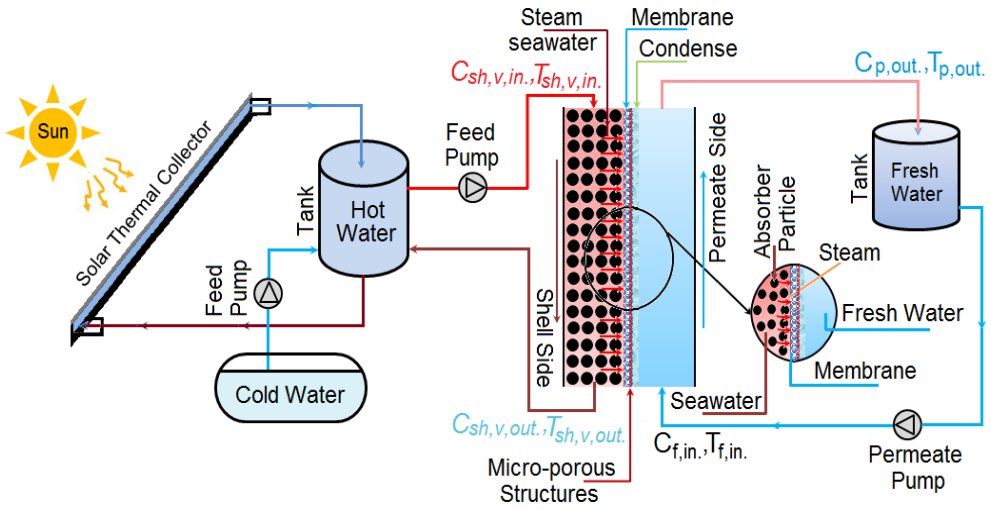

Figure 1. Schematic setup of a solar-driven DCM distillation module.

2.1 Methodology

The schematic setup from Figure 1 is built of solar thermal collector, hot water tank, feed pump, DCM distillation module, fresh water, and permeate pump, respectively. The methodology reported in this work consists of the following steps: (i) data collection, (ii) DCM distillation module modelling, (iii) shell side's model equations on the DCM distillation module, (iv) permeate side's model equations on the DCM distillation module, (v) numerical solution of model equations.

2.2 Data collection

The measured climate data include the solar irradiance, the ambient temperature, and the wind velocity and they were measured for years of 2015 to 2020 in Recife metropolitan region of Pernambuco state. These data were collected for twelve months of each year. Here, authors have chosen only the 2020 year's data to be analyzed. As results, among the 2020 year, authors have selected the hottest months of this year and can be seen in Figure 2 as follows. This study is limited only to the solar radiation flux and has objective to check the solar radiation's effect on the temperature profiles of the DCM distillation module. The Average Solar Radiation Flux (ASRF) of each month has values of G_{ASRF} = 976,102 (February 2020), G_{ASRF} = 972,473 (August 2020), and G_{ASRF} = 837,439 (November 2020), respectively.

- Energy equation for the water steam;

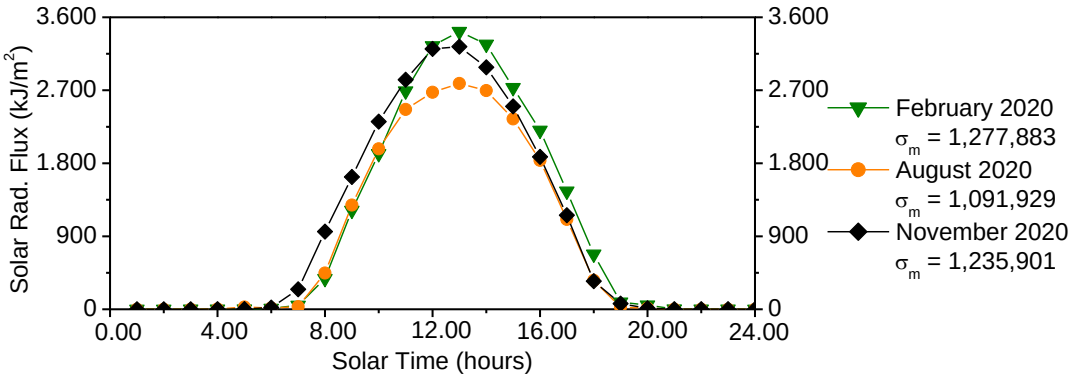

Figure 2. The experimental variations of the solar radiance.

2.3 Direct problem

A schematic setup has been used to develop the mathematical modelling and can be seen in Figure 3 below. This figure shows the detailed steps of a DCM distillation module. Up until now, some works were published on the DCM distillation process (Chen et al., 2021; Alia et al., 2019; Donato et al., 2020), but these works didn't provide theoretical leading to the DCM distillation module on the packed bed. The fluid-solid contact in the packed bed system improves the heat and mass transfer because of the interfacial surface's effect of solid particles. The use of mathematical models can be used to predict the heat and mass physical phenomena in the fluid-solid systems. Thus, it was developed a heterogeneous mathematical model that involves the DCM distillation module's heat and mass transfer equations as follows.

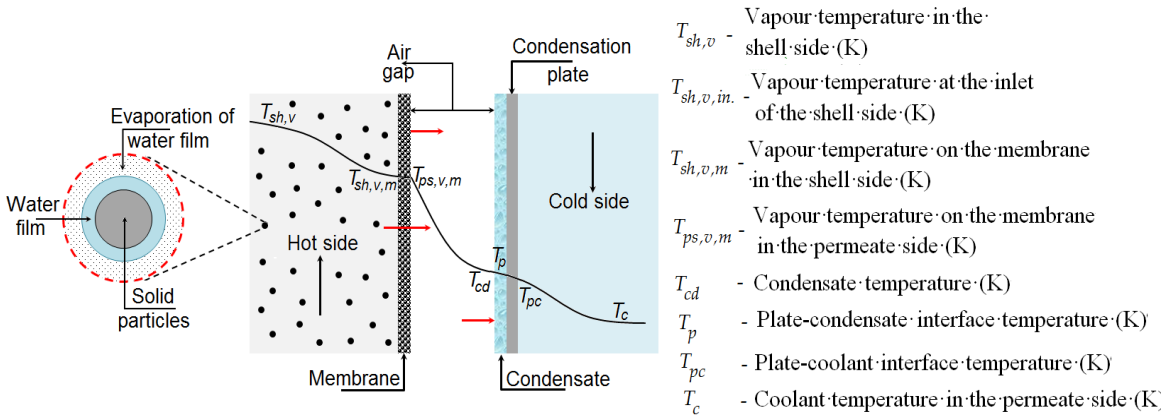

Figure 3. Temperature profile in a DCM distillation module.

2.4 Heat transfer in the shell side

An energy balance equation is developed to describe the water steam's temperature on the DCM distillation module shell side. Thus, the governing energy balance of the water steam is built as follows.

- Energy equation for the water steam;

$$\varepsilon \rho_{sh,v} C_{p,sh,v} \frac{\partial T_{sh,v}}{\partial t} = \lambda_{r,eff,v} \frac{1}{r} \frac{\partial}{\partial r}\left(r \frac{\partial T_{sh,v}}{\partial r} \right) - u_v \rho_{sh,v} C_{p,sh,v} \frac{\partial T_{sh,v}}{\partial z} - h_{vs} A_{is} \left[T_{sh,v} - \left(T_{sh,v,s}\Big|_{r_s = R_s} + \frac{T_{sh,v,m} + T_{ps,v,m}}{2} \right) \right] - \left[\frac{k_m}{\delta_w} \left(T_{sh,v,m} - T_{cd} \right) + J_w H_v \right] \quad (1)$$

- Initial and boundary conditions for Equation (1) are defined as;

$$T_{sh,v}\Big|_{t=0} = T_{sh,v,0} \tag{2}$$

$$T_{sh,v}\Big|_{z=0^+} = T_{sh,v,in.} \tag{3}$$

$$\left.\frac{\partial T_{sh,v}}{\partial z}\right|_{z=L} = 0 \tag{4}$$

$$\left.\frac{\partial T_{sh,v}}{\partial r}\right|_{r=R/2} = \frac{h_{vs}}{\lambda_{r,eff,v}}\left[T_{sh,v} - \left(T_{sh,v,s}\Big|_{r=R} + \frac{T_{sh,v,m} + T_{ps,v,m}}{2}\right)\right] \tag{5}$$

$$\left.\frac{\partial T_{sh,v}}{\partial r}\right|_{r=0} = 0 \tag{6}$$

On the other hand, an energy balance equation is also built up to report the water steam's temperature inside solid particles as follows.

- Energy equation for the water steam in the solid phase

$$(1-\varepsilon)\rho_{sh,s} C_{p,sh,s} \frac{\partial T_{sh,v,s}}{\partial t} = \lambda_{eff,s} \frac{1}{r_s^2}\frac{\partial}{\partial r_s}\left(r_s^2 \frac{\partial T_{sh,v,s}}{\partial r_s}\right) \tag{7}$$

- Initial and boundary conditions for Equation (7) are defined as;

$$T_{sh,v,s}\Big|_{t=0} = T_{sh,v,s,0} \tag{8}$$

$$\left.\frac{\partial T_{sh,v,s}}{\partial r_s}\right|_{r_s=R_s} = \frac{h_{vs}}{\lambda_{eff.,s}}\left(T_{sh,v} - T_{sh,v,s}\Big|_{r_s=R_s}\right) \tag{9}$$

$$\left.\frac{\partial T_{sh,v,s}}{\partial r_s}\right|_{r=0} = 0 \tag{10}$$

2.5 Mass transfer in the shell side

Mass balance equations are constructed to report the dissolved salt's (NaCl) concentration in fluid and solid phases on the DCM distillation module shell side as follows.

- Mass balance for NaCl in fluid phase on the shell side;

$$\varepsilon \frac{\partial C_{sh,NaCl}}{\partial t} = D_{r,eff,NaCl}\frac{1}{r}\frac{\partial}{\partial r}\left(r\frac{\partial C_{sh,NaCl}}{\partial r}\right) - u_{NaCl,avg.}\frac{\partial C_{sh,NaCl}}{\partial z} - k_{NaCl,s}A_{is}\left(C_{sh,NaCl} - C_{sh,NaCl,s}\Big|_{r_s=R_s}\right) \tag{11}$$

- Initial and boundary conditions for Equation (11) are defined as;

$$C_{sh,NaCl}\Big|_{t=0} = C_{sh,NaCl,0} \tag{12}$$

$$C_{sh,NaCl}\Big|_{z=0^+} = C_{sh,NaCl,in.} \tag{13}$$

$$\left.\frac{\partial C_{sh,NaCl}}{\partial z}\right|_{z=L} = 0 \tag{14}$$

$$\left.\frac{\partial C_{sh,NaCl}}{\partial r}\right|_{r=R/2} = \frac{k_{vs}}{D_{r,eff,NaCl}}\left(C_{sh,NaCl} - C_{sh,NaCl,s}\Big|_{r=R}\right) \tag{15}$$

$$\left.\frac{\partial C_{sh,NaCl}}{\partial r}\right|_{r=0} = 0 \tag{16}$$

A mass balance equation has been also developed to describe the dissolved salt's (NaCl) concentration inside solid phase as follows.

- Mass balance for NaCl in solid phase on the shell side;

$$\left(1-\varepsilon\right)\frac{\partial C_{sh,NaCl,s}}{\partial t} = D_{eff,NaCl,s}\frac{1}{r_s^2}\frac{\partial}{\partial r_s}\left(r_s^2\frac{\partial C_{sh,NaCl,s}}{\partial r_s}\right) \tag{17}$$

- Initial and boundary conditions for Equation (17) are defined as;

$$C_{sh,NaCl,s}\Big|_{t=0} = C_{sh,NaCl,s,0} \tag{18}$$

$$\left.\frac{\partial C_{sh,NaCl,s}}{\partial r_s}\right|_{r_s=R_s} = \frac{k_{vs}}{D_{eff,NaCl,s}}\left(C_{sh,NaCl} - C_{sh,NaCl,s}\Big|_{r_s=R_s}\right) \tag{19}$$

$$\left.\frac{\partial C_{sh,NaCl,s}}{\partial r_s}\right|_{r=0} = 0 \tag{20}$$

Mass balance equations are developed to describe the water steam's concentration on the DCM distillation module shell side. Mass balance equation for the water steam's concentration is shown as follows.

- Mass balance for water steam on the shell side;

$$\varepsilon\frac{\partial C_{sh,v}}{\partial t} = D_{r,eff,v}\frac{1}{r}\frac{\partial}{\partial r}\left(r\frac{\partial C_{sh,v}}{\partial r}\right) - u_v\frac{\partial C_{sh,v}}{\partial z} - k_{vs}A_{is}\left[C_{sh,v} - \left(C_{sh,v,s}\Big|_{r_s=R_s} + \frac{C_{sh,v,m}+C_{ps,v,m}}{2}\right)\right] \frac{2\varepsilon P_t}{R_u\left|P_a\right|_{ln}}\frac{D_{w,a}}{\left(\delta_m\tau+b\right)\left(T_{sh,v,m}+T_{cd}\right)}\left(P_{sh,v,m}-P_{cd}\right) \tag{21}$$

- Initial and boundary conditions for Equation (21) are defined as;

$$C_{sh,v}\Big|_{t=0} = C_{sh,v,0} \tag{22}$$

$$C_{sh,v}\Big|_{z=0^+} = C_{sh,v,in.} \tag{23}$$

$$\frac{\partial C_{sh,v}}{\partial z}\Big|_{z=L} = 0 \tag{24}$$

$$\frac{\partial C_{sh,v}}{\partial r}\Big|_{r=R/2} = \frac{k_{vs}}{D_{r,eff,v}}\left[C_{sh,v} - \left(C_{sh,v,s}\Big|_{r_s=R_s} + \frac{C_{sh,v,m}+C_{ps,v,m}}{2}\right)\right] \tag{25}$$

$$\frac{\partial C_{sh,v}}{\partial r}\Big|_{r=0} = 0 \tag{26}$$

Moreover, a mass balance equation is also developed to describe the water vapour's concentration inside solid particles as follows.

- Mass equation for the water steam in the solid phase;

$$(1-\varepsilon)\frac{\partial C_{sh,v,s}}{\partial t} = D_{eff,v,s}\frac{1}{r_s^2}\frac{\partial}{\partial r_s}\left(r_s^2\frac{\partial C_{sh,v,s}}{\partial r_s}\right) \tag{27}$$

- Initial and boundary conditions for Equation (27) are defined as;

$$C_{sh,v,s}\Big|_{t=0} = C_{sh,v,s,0} \tag{28}$$

$$\frac{\partial C_{sh,v,s}}{\partial r_s}\Big|_{r_s=R_s} = \frac{k_{vs}}{D_{eff,v,s}}\left(C_{sh,v} - C_{sh,v,s}\Big|_{r_s=R_s}\right) \tag{29}$$

$$\frac{\partial C_{sh,v,s}}{\partial r_s}\Big|_{r=0} = 0 \tag{30}$$

There are complementary equations in Equations (1)-(30). These equations are used to supplement the mathematical model's energy and mass equations and can be found in Equations (31)-(41) below.

$$T_{sh,v,m} = T_{sh,v} - \frac{H}{h_{vs}}\left[\left(T_{sh,v} - T_c\right) + \frac{J_w H_v}{h^*}\right] \tag{31}$$

$$T_{cd} = T_c + \frac{H}{h_p}\left[\left(T_{sh,v} - T_c\right) + \frac{J_w H_v}{h^*}\right] \tag{32}$$

$$J_w = \frac{2\varepsilon P_t D_{w,a}\left(P_{sh,v,m,salt} - P_{cd}\right)}{R\left|P_a\right|_{ln}\left(\delta_m \tau + b\right)\left(T_{sh,v,m} + T_{cd}\right)} \tag{33}$$

$$\left|P_a\right|_{ln} = \frac{\left(P_{a,sh,v,m} - P_{a,cd}\right)}{ln\left(\frac{P_{a,sh,v,m}}{P_{a,cd}}\right)} \tag{34}$$

$$P_{a,sh,v,m} = P_t - P_{sh,v,m,salt} \tag{35}$$

$$P_{a,cd} = P_t - P_{cd} \tag{36}$$

$$P_{sh,v,m} = exp\left(23.196 - \frac{3816.44}{T_{sh,v,m} - 46.13}\right) \tag{37}$$

$$P_{cd} = exp\left(23.196 - \frac{3816.44}{T_{cd} - 46.13}\right) \tag{38}$$

$$P_{sh,v,m,salt} = \left(1 - C_{sh,NaCl}\right)P_{sh,v,m} \tag{39}$$

$$C_{sh,v,m} = \frac{P_{sh,v,m} M}{R_u T_{sh,v,m}} \tag{40}$$

$$C_{ps,v,m} = \frac{\delta_m \tau}{L_m}\frac{P_{sh,v,m} M}{R_u T_{sh,v,m}} \tag{41}$$

2.6 Permeate side

The amount of permeated water depends not only on the membrane properties, but it is also a temperature function in the permeation side. Thus, an energy balance was developed on the permeation side as follows.

- Mass equation in the permeation side;

$$d\rho_c u_c C_{p,c}\frac{dT_c}{dz} = \frac{2 r_0 R_u J_w}{M_c r_i^2}\left(T_{sh,v,m} - T_c\right) \tag{42}$$

- Boundary conditions for Equation (42) are defined as;

$$T_c\Big|_{z=0^+} = T_{c,in.} \tag{43}$$

$$\left.\frac{dT_c}{dz}\right|_{z=L} = 0 \tag{44}$$

2.7 Numerical solution of the direct problem

The numerical solution of the mathematical model was carried out for a numeric method which ensures numerical stability (Cruz and Abreu, 2017). The proposed model was solved by the finite volume method (FVM) in together with prescribed initial and boundary conditions to analyze the performance of the DCM distillation module.

3. RESULTS AND DISCUSSIONS

The mathematical modelling was used to investigate the performance from DCM distillation module using the solar energy's thermal energy. The physical parameters used to obtain the results are shown in Table 1 as follows.

Table 1. Physical parameters used to obtain the simulation results.

Parameters	VALUES
Steam density ($\rho_{sh,\,v}$), kg/m^3	0.989
Void fraction (ε), $m^3 vapor/m^3\ distillation$	0.92
Radial steam thermal cond. ($\lambda_{r,eff,\,v}$), W/mK [(1)]	0.083
Steam cap. in the shell side ($C_{P,\,sh,\,v}$), kJ/kgK [(1)]	1.043
Steam velocity (u_v), $m/sec.$	0.147
Steam-solid heat transfer coef. (h_{vs}), $W/m^2 sec.$ [(1)]	120
Interphase specific surface area (A_{is}), $1/m$	1600
Thermal cond. of the membrane (k_m), $W/m\ K$	0.101
Membrane thickness (δ_m), µm	0.35
Solid thermal conductivity ($\lambda_{eff,\,s}$), W/mK	0.150
Gas constant (R_u), $kJ/K\ kmol$	8.314
Operating pressure ($P_{op.}$), kPa	101.325
Solid density ($\rho_{sh,\,s}$), kg/m^3	1400
Solid cap. in the shell side ($C_{P,\,sh,\,s}$), kJ/kgK [(1)]	0.650
Radial dispersion coef. of NaCl ($D_{r,\,eff,\,NaCl}$), $m^2/sec.$	4.251×10^{-5}
Salt particles's average velocity ($u_{NaCl,\,avg.}$), $m/sec.$	0.197
Mass transfer coef. of NaCl ($k_{NaCl,\,s}$), $m/sec.$	6.982×10^{-3}
Dispersion coef. of NaCl in the solid phase ($D_{r,\,eff,\,NaCl,\,s}$), $m^2/sec.$	9.83×10^{-7}
Radial dispersion coef. of steam ($D_{r,eff,\,v}$), $m^2/sec.$ [(1)]	1.673×10^{-4}
Steam-solid mass transfer coef. ($k_{v,\,s}$), $m/sec.$	3.023×10^{-2}
Steam dispersion coef. in the solid phase ($D_{eff,\,v,\,s}$), $m^2/sec.$ [(1)]	5.012×10^{-5}
Tortuosity (τ), (-)	2.0
Heat cap. in the permeate side ($C_{P,\,c}$), kJ/kgK [(1)]	10.723
Velocity in the permeate side (u_c), $m/sec.$	0.209

[(1)] measured at 90°C

3.1 Validation and numerical experiments

To assure the validity of the developed model, it is necessary to compare the simulating results with corresponding literature data. The simulating results are computed from a computer code developed by authors. Figure 4 compares the literature data and simulated results of the J_W under different feed temperature. The experimental data of the J_W obtained for Elhenawy et al. (2020) are compared to simulated results from the J_W with particles and without particles.

Figure 5 shows the water vapour's temperature profiles in the shell side with particles and without particles to three different feed temperatures. As it was described in Section 2, the feed temperatures at the DCM distillation module's shell side are obtained in respect to ASR flux of each month, i.e., 976.102 (T_{feed} = 94 °C), 972.473 (T_{feed} = 90 °C), and 837.439 (T_{feed} = 86 °C), respectively.

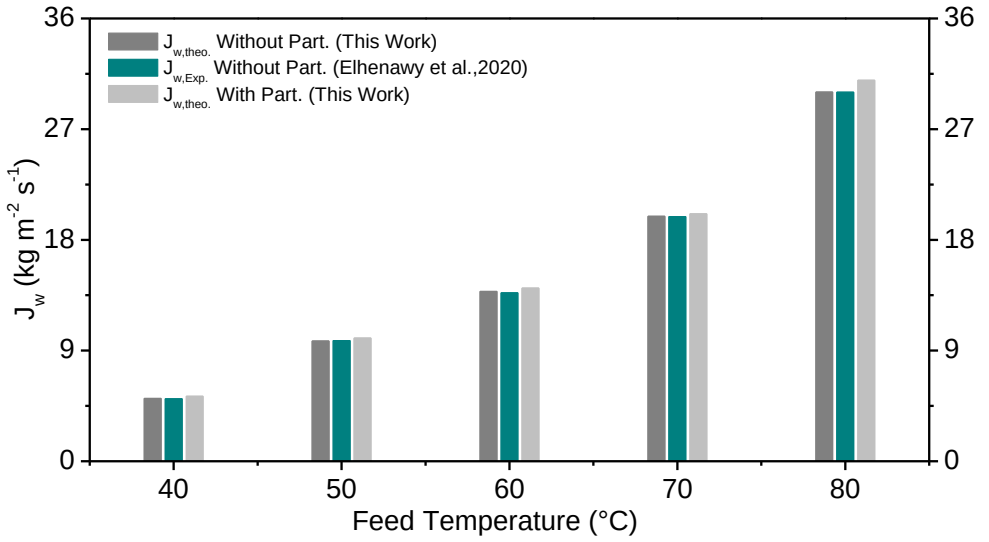

Figure 4. Comparison of results from the J_W.

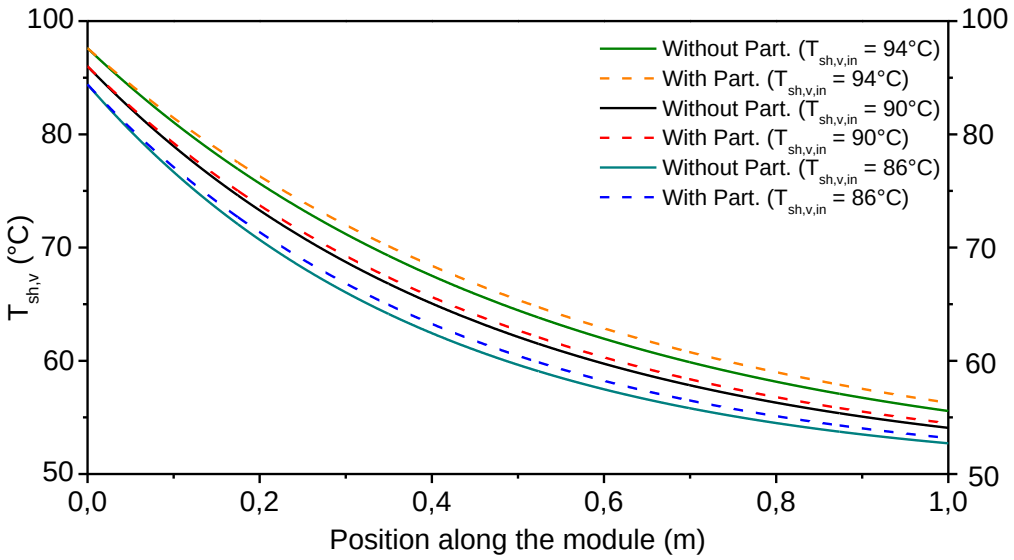

Figure 5. Comparison of $T_{sh,v}$ with and without particles.

4. CONCLUSIONS

This study has been focused on the physical-mathematical modelling of the heat and mass transfer for a DCM distillation module. An analysis to describe the performance of the permeate flux (J_W) and water vapour's temperature profiles is carried out and can be summarized the following conclusions:

1. A satisfactory agreement has been shown between the experimental data of the J_W and results of this work. At the temperature of 80 °C, the value of the J_W with particles was higher.
2. The DCM distillation module's shell side when filled with particles increases the temperature profiles of the water vapour due to improvement on the heat transfer.

5. ACKNOWLEDGEMENTS

The authors are grateful to University of Pernambuco for the financial support given (Project 127/2019).

6. REFERENCES

Ali, A., Tufa, R. A., Macedonio, F., Curcio, E. and Drioli E., 2018. "Membrane technology in renewable-energy-driven desalination". *Renewable and Sustainable Energy Reviews*, Vol. 81, pp. 1-21.

Chen, Y-H., Hung, H-G., Ho, C-D. and Chang H., 2021. "Economic design of solar-driven membrane distillation systems for desalination". *Membranes*, Vol. 11, pp. 1-20.

Cruz, B. M. and Silva, J. D., 2017. "A two-dimensional mathematical model for the catalytic steam reforming of methane in both conventional fixed-bed and fixed-bed membrane reformers for the production of hydrogen". *International Journal of Hydrogen Energy*, Vol. 42, pp. 23670-23690.

Donato, L., Garofalo, A., Drioli, E., Alharbi, O., Aljlil, S. A., Criscuoli, A. and Algieri, C., 2020. "Improved performance of vacuum membrane distillation in desalination with zeolite membranes". *Separation and Purification Technology*, Vol. 237, pp. 116376.

Elhenawy, Y., Elminshawy, N. A. S., Bassyouni, M., Alanezi, A. and Drioli, E., 2020. "Experimental and theoretical investigation of a new air gap membrane distillation module with a corrugated feed channel". *Journal of Membrane Science*, Vol. 594, pp. 117461.

Golubev, G., Eremeev, I., Makaev, S., Shalygin, M., Vasilevsky, V., He, T., Drioli, E. and Volkov, A., 2021. "Thin-film distillation coupled with membrane condenser for brine solutions concentration". Desalination, Vol. 503, p. 114956.

Kalogirou, S. A., 2005. "Seawater desalination using renewable energy sources". *Progress in Energy and Combustion Science*, Vol. 31, pp. 242-281.

Rafiei, A., Loni, R., Mahadzir, S. B., Najafi, G., Pavlovic, S. and Bellos, E., 2020. "Solar desalination system with a focal point concentrator using different nanofluids". *Applied Thermal Engineering*, Vol. 174, p.115058.

Voltolina, S., Marín, P., Díz, F. V. and Salvador, O., 2017. "Open-cell foams as beds in multiphase reactors: Residence time distribution and mass transfer". *Chemical Engineering Journal*, Vol. 316, pp. 323 - 331.

Ying, L., Zhu, H., Huang, H., Qu, X., Wang, C., Wang, X., Duan, F., Lu, S. and Du M., 2021. "Scalable $N_iCo_xS_y$-PANI@GF Membranes with Broadband Light Absorption and High Salt-Resistance for Efficient Solar-Driven Interfacial Evaporation". *ACS Applied Energy Materials*, Vol. 4, pp. 3563-3572.

7. RESPONSIBILITY NOTICE

The author(s) is (are) the only responsible for the printed material included in this paper.